X-ray Absorption Spectroscopy of Cuprous–Thiolate Clusters in Proteins and Model Systems

Ingrid J. Pickering,[†] Graham N. George,*[,†] Charles T. Dameron,[‡] Boris Kurz,[‡] Dennis R. Winge,[‡] and Ian G. Dance[§]

Contribution from the Stanford Synchrotron Radiation Laboratory, Stanford University, SLAC, P.O. Box 4349, Bin 69, Stanford, California 94309, Departments of Medicine and Biochemistry, University of Utah Medical Center, Salt Lake City, Utah 84132, and School of Chemistry, University of New South Wales, Kensington, NSW 2033, Australia

Received April 12, 1993[⊗]

Abstract: Cuprous–thiolate multimetallic clusters exist in a range of different biological molecules for which no structural information exists from X-ray crystallography. Spectroscopic tools such as X-ray absorption spectroscopy have provided the major structural insights into this family of biological molecules. Recent nuclear magnetic resonance data on silver-substituted metallothionein, thought to be analogous with the copper proteins, have suggested the presence of digonal coordination [Narula, S. S.; Mehra, R. K.; Winge, D. R.; Armitage, I. M. *J. Am. Chem. Soc.* **1991**, *113*, 9354–9358]. In order to test this in the copper case, we have examined a series of structurally characterized cuprous–thiolate model compounds, containing different proportions of digonal and trigonal copper sites, using copper K-edge X-ray absorption spectroscopy. The edge spectra, which have been previously used as a probe for the average copper coordination environment in proteins, show little variation between the models, indicating that these are not useful as a probe of coordination environment in the case of cuprous–thiolate clusters (as opposed to isolated metal sites). We show that systematic trends in the average Cu–S bond length from EXAFS curve-fitting analysis can be used to obtain an estimate of the fraction of digonal and trigonal copper sites. This correlation is applied to a series of different proteins containing cuprous–thiolate clusters which are found to contain significant fractions of digonal copper.

Introduction

Proteins containing cuprous–thiolate multimetallic clusters form a family of biological molecules for which structural information from crystallography is lacking. Structural information has, however, been obtained from spectroscopic techniques such as X-ray absorption spectroscopy (XAS; see *e.g.* ref 1 and references therein). Copper metallothioneins have been intensively studied and can be considered to be prototypical cuprous–thiolate proteins.[1] Metallothioneins are small, cysteine-rich polypeptides which bind metal ions such as copper and zinc. In copper metallothioneins, the cysteine thiolates bridge the cuprous ions to form a multimetallic cluster.[2,3]

Cuprous–thiolate multimetallic cluster proteins have diverse functions in a variety of organisms. In yeast, the function of metallothioneins is to buffer the cellular cytoplasm of copper ions in order to minimize copper-induced toxicity.[4] The fission yeast *Schizosaccharomyces pombe* does not contain metallothionein; a physiologically equivalent role is fulfilled by the formation of cuprous–thiolate multimetallic clusters coated with glutathione-related isopeptides.[5] A similar function of buffering intracellular metal levels has been postulated for metallothionein in animal cells, although direct roles remain to be established.[6,7] Some DNA-binding proteins also contain cuprous–thiolate multimetallic clusters.[8-10] Yeast regulate the production of metallothionein by responding to the levels of copper or silver present in the growth medium.[6,8,11-14] This is done at the level of DNA transcription by intracellular copper sensor protein molecules which stimulate the transcription of the metallothionein gene in the presence of copper ions.[8,13,14] In the case of the yeast *Saccharomyces cerevisiae*, the formation of a multimetallic cuprous–thiolate cluster in the copper sensor protein (known as the ACE1, or CUP2, transcription factor[8,13]) is required to activate the expression of metallothionein genes.[8-10] A closely homologous protein, AMT1, identified in *Candida glabrata*, mediates the expression of a family of metallothionein genes in this yeast.[11,15] The activation of ACE1 and AMT1 is specific for Cu(I) and Ag(I) ions.[8-10] The oncogenic protein E7 from the *Papilloma* virus is capable of forming a cuprous–thiolate cluster, although it is not clear whether the physiological role is fulfilled by a copper- or zinc-substituted protein.[16] Perhaps most significantly, a deficiency in a metallothionein-like protein was recently implicated as a possible cause of Alzheimer's syndrome.[17] The role of the metal clusters in this novel protein is currently under study.

[†] Stanford Synchrotron Radiation Laboratory.
[‡] University of Utah.
[§] University of New South Wales.
[⊗] Abstract published in *Advance ACS Abstracts*, September 15, 1993.

(1) Winge, D. R.; Dameron, C. T.; George, G. N. *Adv. Inorg. Biochem.*, in press.
(2) (a) George, G. N.; Byrd, J.; Winge, D. R. *J. Biol. Chem.* **1988**, *263*, 8199–8203. (b) George, G. N.; Winge, D. R.; Stout, C. D.; Cramer, S. P. *J. Inorg. Biochem.* **1986**, *27*, 213–220.
(3) Narula, S. S.; Mehra, R. K.; Winge, D. R.; Armitage, I. M. *J. Am. Chem. Soc.* **1991**, *113*, 9354–9358.
(4) (a) Hamer, D. H.; Thiele, D. J.; Lemontt, L. E. *Science* **1985**, *228*, 685–690. (b) Wright, C. F.; Hamer, D. H.; McKenney, K. *J. Biol. Chem.* **1968**, *263*, 1570–1574. (c) Ecker, D. J.; Butt, T. R.; Sternberg, E. J.; Neeper, M. P.; Debouck, C.; Gorman, J. A.; Crooke, S. T. *J. Biol. Chem.* **1986**, *261*, 16895–16900.
(5) Reese, R. N.; Mehra, R. K.; Tarbet, E. B.; Winge, D. R. *J. Biol. Chem.* **1988**, *263*, 4186–4192.
(6) Hamer, D. H. *Annu. Rev. Biochem.* **1986**, *55*, 913–951.
(7) Bremner, I. *Experientia, Suppl.* **1987**, *52*, 81–104.
(8) (a) Furst, P.; Hu, S.; Hackett, R.; Hamer, D. H. *Cell* **1988**, *55*, 705–717. (b) Thiele, D. J. *Mol. Cell. Biol.* **1988**, *8*, 2745–2752.
(9) Dameron, C. T.; Winge, D. R.; George, G. N.; Sansone, M.; Hu, S.; Hamer, D. *Proc. Natl. Acad. Sci. U.S.A.* **1991**, *88*, 6127–6131.
(10) Nakagawa, K. H.; Inouye, C.; Hedman, B.; Karin, M.; Tullius, T. D.; Hodgson, K. O. *J. Am. Chem. Soc.* **1991**, *113*, 3621–3623.
(11) Zhou, P.; Thiele, D. J. *Proc. Natl. Acad. Sci. U.S.A.* **1991**, *88*, 6112–6116.
(12) Thiele, D. J. *Nucleic Acids Res.* **1992**, *20*, 1183–1191.
(13) Welch, J.; Fogel, S.; Buchman, C.; Karin, M. *EMBO J.* **1989**, *8*, 255–260.
(14) Hu, S.; Furst, P.; Hamer, D. *New Biol.* **1990**, *2*, 544–555.
(15) Zhou, P.; Szczypka, M. S.; Sosinowksi, T.; Thiele, D. J. *Mol. Cell. Biol.* **1992**, *12*, 3766–3775.
(16) Roth, E. J.; Kurz, B.; Liang, L.; Hansen, C. L.; Dameron, C. T.; Winge, D. R.; Smotkin, D. *J. Biol. Chem.* **1992**, *267*, 16390–16395.

0002-7863/93/1515-9498$04.00/0

In all known cases, the copper ions are present as Cu(I) and the sulfur ligands are provided by cysteinyl sulfurs. Proteins and peptides containing cuprous–thiolate clusters are known to have an abundance of cysteine residues,[1,5,6,8,18,19] with a common sequence motif being Cys-X-Cys or Cys-X-X-Cys in which X represents any other amino acid. The conserved cysteinyl residues are very likely the ligands of the copper multimetallic cluster. No complete structures are as yet available for copper–thiolate multimetallic clusters in proteins. Nevertheless, strong chemical precedence exists for multimetallic copper–thiolate species.[20] X-ray crystal structures of several synthetic cuprous–thiolate multimetallic clusters have been determined.[20] Different stoichiometries have been characterized, including Cu_3S_3, Cu_4S_4, Cu_4S_6, Cu_5S_6, Cu_5S_7, Cu_6S_8, Cu_8S_8, Cu_8S_{12}, and $Cu_{12}S_{12}$.[20-30] In all of these clusters the copper possesses a formal cuprous oxidation state. Analysis of the structural features of these clusters has led to a number of generalizations. Thiolate ligands tend to maintain low coordination numbers of Cu(I), and both digonal and trigonal coordination stereochemistries are common, sometimes coexisting in one cluster. The thiolate ligands are predominantly doubly-bridging (*i.e.* coordinated to two metals), and these thiolate bridges, rather than copper–copper bonds, are the principal cohesive force in the clusters.

A limited number of spectroscopic techniques are available which can provide structural information for multimetallic clusters. Two of these are X-ray absorption spectroscopy (XAS) and high-resolution NMR. These provide complementary information; XAS can provide local structural information with very accurate interatomic distances, but somewhat poor estimates of coordination number and scatterer size (atomic number), whereas high-resolution NMR can, in some cases, provide an entire structure, although bond distances are less accurately determined. Although both naturally abundant isotopes of copper (^{63}Cu and ^{65}Cu) are magnetic with $I = {}^3/_2$ and similar magnetic moments, the presence of nuclear quadrupole effects makes NMR less useful for this element. Recently, heteronuclear (^1H–^{109}Ag) multiple quantum coherence NMR studies performed on silver metallothionein from *S. cerevisiae* established the connectivities of ten cysteinyl residues with seven bound $^{109}Ag(I)$ ions.[3] Ag(I) is isoelectronic with Cu(I), and their metal–thiolate compounds and thiolate clusters show similar structural principles; silver metallothionein is likely to be isostructural with copper metallothionein. In the case of metallothionein, there is good evidence that the silver and copper proteins are structurally very similar,[3] although in general caution should be exercised in extrapolating structural information on silver proteins to copper proteins, as Ag–S bonds are typically more than 0.2 Å longer than Cu–S bonds. Narula *et al.*[3] questioned the original proposal from XAS of a Cu_8S_{12} cluster stoichiometry with trigonal Cu(I) coordination.[2] On the basis of the NMR results, a new model cluster M_7S_{10} (M = Cu or Ag) was proposed, in which two of the seven metal ions may exist in digonal coordination, with the remainder in trigonal coordination.[3]

The suggestion of possible digonal Ag(I) ions in yeast silver metallothionein by NMR has prompted us to reevaluate the XAS data from proteins containing cuprous–thiolate clusters. The question addressed is whether XAS can detect mixed-coordination complexes in multimetallic cuprous–thiolate complexes. In this report, we present XAS data on a series of synthetic cuprous–thiolate multimetallic clusters containing different proportions of digonal and trigonal copper, together with new data on a series of cuprous–thiolate proteins. Figure 1 shows the crystal structures of the copper–sulfur cluster cores of the three model compounds used in this study.[21,23,25,26] The trends observed from these models provide new insights into the copper coordination for the protein systems and are used in the interpretation of the XAS of a number of different copper–thiolate proteins.

Materials and Methods

Sample Preparation. The compounds bis(tetramethylammonium) hexakis(μ-benzenethiolato)tetracuprate(I), $(Me_4N)_2[Cu_4(SPh)_6]$ (or Cu_4S_6),[21,23,31] bis(tetramethylammonium) heptakis(μ-benzenethiolato)-pentacuprate(I), $(Me_4N)_2[Cu_5(SPh)_7]$ (or Cu_5S_7),[26] and tetraethylammonium hexakis(μ-thiolato)pentacuprate(I), $(Et_4N)[Cu_5(SBu^t)_6]$ (or Cu_5S_6),[25] were prepared and characterized as previously described. Samples for X-ray absorption spectroscopy were finely ground under anaerobic conditions and appropriately diluted with boron nitride, after which the mixture was packed into aluminum holders of 1-mm path length with thin Mylar windows.

Yeast copper metallothionein from *S. cerevisiae* was isolated from cultures grown in the presence of 1 mM $CuSO_4$ and purified as previously reported.[19] Purified copper metallothionein contained 7–8 mol equiv of Cu(I). The N-terminal half ACE1 from *S. cerevisiae* was purified from a T7 *Escherichia coli* expression system as described previously.[9] Metal-free ACE1 was prepared and the fully reduced sample was used for Cu(I) reconstitution.[9] Cu(I) was titrated into ACE1 according to the published protocol,[9] except that reduced glutathione was mixed with the metal-free ACE1 to a final concentration of 5 mM prior to addition of 6.8 mol equiv of Cu(I). The Cu:protein stoichiometry was verified using atomic absorption spectrophotometry and amino acid analysis. The integrity of the CuACE1 complex was verified by quantifying UV–visible fluorescence emission spectra,[9] which were found to be consistent with fully metalated ACE1.[9]

Cu(I)–γEC peptide complexes from *S. pombe* were isolated from cultures grown in the presence of 1 mM $CuSO_4$ as described previously.[5] Ligands for the Cu(I) complexes are provided by the cysteinyl thiolates of glutathione-related isopeptides of general sequence $(\gamma EC)_nG$ where n typically varies from 2 to 4. The actual M_r of the complex is unknown, but the apparent M_r is consistent with an oligomeric structure, $Cu_x[(\gamma EC)_nG)]$, containing a polymetallic cluster. Synthetic $(EC)_nG$ peptides were synthesized by solid-phase peptide synthesis with either α peptide linkages, $(EC)_3G$, or the isopeptide variant $(\gamma EC)_nG$ using an Applied Biosystems (ABI) 431A peptide synthesizer on (*p*-(hydroxymethyl)phenoxy)methyl resin. The synthesis was carried out in the presence of 1-hydroxybenzotriazole and *N*,*N*-dicyclohexylcarbodiimide with N-FMOC-glycine (ABI), N-FMOC-L-cysteine-Trt (ABI), N-FMOC-L-glutamic acid γ-*tert*-butyl ester (ABI), and N-FMOC-L-glutamic acid α-*tert*-butyl ester (Bachem) using *N*-methylpyrrolidone as the solvent. Peptides were cleaved from the resin and side chains deblocked at room temperature with 95% TFA, 2.5% water, and 2.5% ethanedithiol. After the cleavage products were dried using a rotary evaporator, the samples were resuspended in 5% acetic acid and purified by preparative C_{18} reverse-phase HPLC in 0.1% TFA and a linear gradient of acetonitrile. The isolated peptides were quantified by amino acid analysis. The Cu(I) complexes with the synthetic peptides were formed with 1.5 mol equiv of Cu(I) per peptide. Cu(I) was stabilized in solution by anaerobically dissolving CuCl in 0.1 N HCl in the presence of 4% NaCl, and this

(17) (a) Uchida, Y.; Takio, K.; Titani, K.; Ihara, Y.; Tomonaga, M. *Neuron* **1991**, *7*, 337–347. (b) Palmiter, R. D.; Findley, S. D.; Whitmore, T. E.; Durnam, D. M. *Proc. Natl. Acad. Sci. U.S.A.* **1992**, *89*, 6333–6337.

(18) Kagi, J. H. R.; Schaffer, A. *Biochemistry* **1988**, *27*, 8509–8515.

(19) Winge, D. R.; Nielson, K. B.; Gray, W. R.; Hamer, D. H. *J. Biol. Chem.* **1985**, *260*, 14464–14470.

(20) Dance, I. G. *Polyhedron* **1986**, *5*, 1037–1104.

(21) Dance, I. G.; Calabrese, J. C. *Inorg. Chim. Acta* **1976**, *19*, L41–L42.

(22) Coucouvanis, D.; Murphy, C. N.; Kanodia, S. K. *Inorg. Chem.* **1980**, *19*, 2993–2998.

(23) Dance, I. G.; Bowmaker, G. A.; Clark, G. R.; Seadon, J. K. *Polyhedron* **1983**, *2*, 1031–1043.

(24) Nicholson, J. R.; Abrahams, I. L.; Clegg, W.; Garner, C. D. *Inorg. Chem.* **1985**, *24*, 1092–1096.

(25) Bowmaker, G. A.; Clark, G. R.; Seadon, F. J. K.; Dance, I. G. *Polyhedron* **1984**, *3*, 535–544.

(26) Dance, I. G. *Aust. J. Chem.* **1978**, *31*, 2195–2206.

(27) Hollander, F. J.; Coucouvanis, D. *J. Am. Chem. Soc.* **1974**, *96*, 5646–5648.

(28) Birker, P. J. M. L.; Freeman, H. C. *J. Am. Chem. Soc.* **1977**, *99*, 6890–6899.

(29) (a) Dance, I.; Fischer, K.; Lee, G. In *Metallothioneins, Synthesis, Structure and Properties of Metallothioneins, Phytochelatins and Metal Thiolate Complexes*; Stillman, M. J., Shaw, C. F., III, Suzuki, K. T., Eds.; VCH: New York, 1992; Chapter 13. (b) Tang, K.; Tang, Y. In *Heteroatom Chemistry*; Block, E., Ed.; VCH: New York, 1990; Chapter 20. (c) Tang, Q.; Tang, K.; Liao, H.; Han, Y.; Chen, Z.; Tang, Y. *J. Chem. Soc., Chem. Commun.* **1987**, 1076–1077.

(30) Throughout this paper S refers to cysteinyl or thiolate sulfur.

(31) Bowmaker, G. A.; Tan, L.-C. *Aust. J. Chem.* **1979**, *32*, 1443–1452.

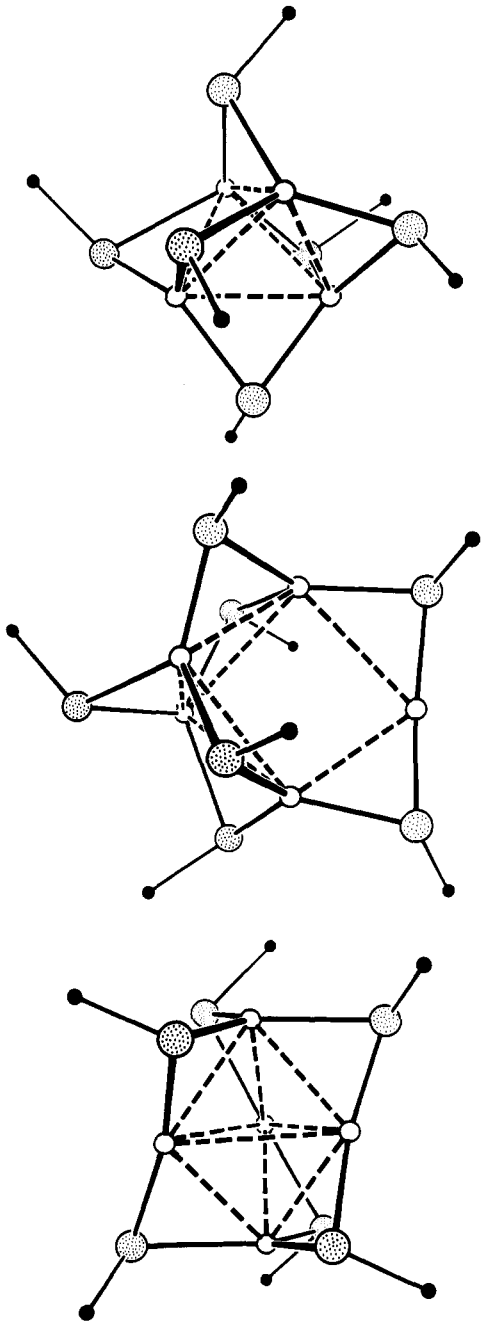

Figure 1. Structures of cuprous–thiolate cluster model compounds. Top: $(Me_4N)_2[Cu_4(SPh)_6]$ (or Cu_4S_6) has exclusively trigonal coordination of the Cu(I) by sulfur and adopts a tetrahedral arrangement of copper atoms. Middle: $(Me_4N)_2[Cu_5(SPh)_7]$ (or Cu_5S_7) has a single digonally coordinated Cu(I), with the remainder in trigonal coordination. Bottom: $(Et_4N)[Cu_5(SBu^t)_6]$ (or Cu_5S_6) has two trigonal and three digonally coordinated coppers. The three compounds therefore form a series with increasing proportions of digonal coordination.

solution was used immediately. No glutathione was included in the reconstitution. Samples for X-ray absorption spectroscopy were prepared with 15% glycerol and frozen in lucite cuvettes with thin Mylar windows. The final copper concentration was close to 3 mM.

CuE7 was prepared as Cu_3E7 as described previously.[16] UV–visible fluorescence emission spectra were used to verify that complex formation had occurred.

XAS Data Collection and Analysis. Copper K-edge X-ray absorption spectra were collected on beamline SB07-3 (1.8 T wiggler field) at the Stanford Synchrotron Radiation Laboratory, with the storage ring SPEAR operating at 3 GeV with ring currents of 50–100 mA. Si(220) monochromator crystals were used, with an upstream vertical aperture of 1 mm, and no focusing optics were present. The monochromator crystals were 50% detuned at the absorption edge, in order to reject harmonics.

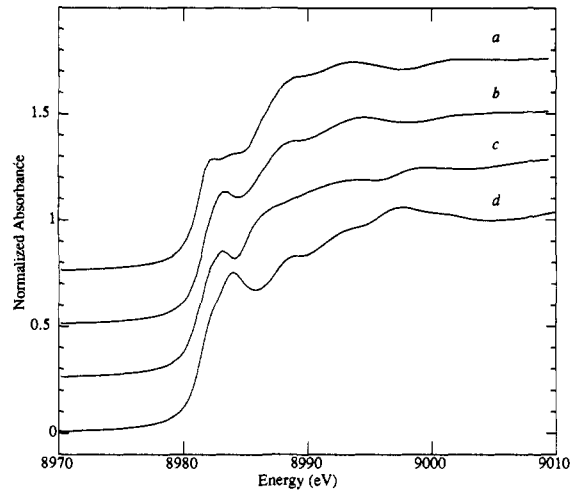

Figure 2. Cu K-edge absorption spectra of model compounds: (a) Cu_4S_6; (b) Cu_5S_7; (c) Cu_5S_6; (d) $Cu(tmtu)_3$.

X-ray absorption was monitored either by recording the Cu Kα fluorescence excitation spectrum using a Canberra 13-element Ge array detector[32] or by measuring the X-ray transmittance using nitrogen-filled ionization chambers. The former was used in the case of the protein samples, and the latter for the model compounds. Samples were held at a constant temperature in the range 4–8 K using an Oxford Instruments CF1204 liquid helium flow cryostat. Energy calibration was carried out by simultaneously recording the spectrum of copper metal, assuming 8980.3 eV for the lowest energy K-edge inflection. Calibrations are considered accurate to better than 0.5 eV. The extended X-ray absorption fine structure (EXAFS) oscillations $\chi(k)$ were quantitatively analyzed by a curve-fitting procedure[33] with the following approximate expression:

$$\chi(k) \simeq \sum_{i=1}^{n} \frac{N_i A_i(k,R_i)}{kR_i^2} \exp\left(\frac{-2R_i}{\lambda(k,R_i)}\right) \exp(-2\sigma_i^2 k_i^2) \times \sin[2kR_i + \phi(k,R_i)] \quad (1)$$

Here k is the photoelectron wavenumber and N_i is the number of i-type atoms at a mean distance R_i from the absorber atom (in this case copper). The summation is over all sets of equivalent atoms, n. The functions $A(k,R_i)$, $\lambda(k,R_i)$, and $\phi(k,R_i)$ are the curved-wave total EXAFS amplitude, photoelectron mean free path, and total EXAFS phase functions, respectively. For the first-shell Cu–S contacts, these functions were calculated in the single-scattering approximation using the program FEFF (version 5.04) of Rehr and co-workers.[34] The value of ΔE_0, a small correction to the energy for $k = 0$ (routinely chosen at the arbitrary value of 9000 eV), was determined to be −12.3 eV from an initial refinement of the Cu_4S_6 cluster data and was held constant at this value for all other fits. For the Cu–Cu outer shells, single-scattering theory did not yield particularly good fits, and the phase and amplitude functions were instead extracted from the Cu_4S_6 cluster data in the following way. The Cu–S shell was fitted, and then a residual spectrum was calculated. The residual spectrum was Fourier transformed, the scatter peak due to the Cu–Cu shell was filtered and back-transformed, and the phase and amplitudes were then extraced assuming $N = 3$, $R = 2.740$ Å, and $\sigma^2 = 0.0075$ Å^2.

In the case of unknown spectra, data were fitted by testing combinations of different interactions, including Cu–S, Cu–N, and Cu–Cu. The best combinations were then chosen for further refinement.

Results

Cu K-Edge XAS of Synthetic Cuprous–Thiolate Cluster Model Compounds. Copper K-edge X-ray absorption edge spectra of the three synthetic Cu(I)–thiolate clusters of stoichiometries Cu_4S_6, Cu_5S_7, and Cu_5S_6 are shown in Figure 2. Also included

(32) Cramer, S. P.; Tench, O.; Yocum, M.; George, G. N. *Nucl. Instrum. Methods Phys. Res.* **1988**, *A266*, 586–591.

(33) George, G. N.; Kipke, C. A.; Prince, R. C.; Sunde, R. A.; Enemark, J. H.; Cramer, S. P. *Biochemistry* **1989**, *28*, 5075–5080.

(34) (a) Rehr, J. J.; Mustre de Leon, J.; Zabinsky, S. I.; Albers, R. C. *J. Am. Chem. Soc.* **1991**, *113*, 5135–5140. (b) Mustre de Leon, J.; Rehr, J. J.; Zabinsky, S. I. *Phys. Rev. B.* **1991**, *44*, 4146–4156.

for comparison is the spectrum of $Cu(tmtu)_3BF_4$,[35] which contains an isolated Cu(I) atom in trigonal planar coordination by the uncharged ligand tetramethylthiourea (tmtu). As expected for formally Cu(I) complexes, none of the spectra show observable 1s → 3d transitions at about 8978 eV. The four spectra are quite similar, with a pronounced feature at about 8984 eV having only subtle (but significant) differences in structure and intensity.

At first sight, this result seems at odds with the previous work of Kau *et al.*[36] In a comprehensive study of Cu(I) and Cu(II) X-ray absorption edges, these workers[36] observed that the 8984-eV peak was a sensitive indicator of Cu(I) coordination, the peak being most intense for digonal and least intense for tetragonal copper coordination. This peak was assigned as the formally dipole-allowed 1s → 4p transition, and the data were rationalized from the expected degeneracy of the 4p orbital from simple ligand field arguments.[36] The studies of Kau *et al.*,[36] however, did not include digonal Cu(I) complexes with thiolate ligands, nor did these workers examine the spectra of cuprous–thiolate clusters with mixed digonal and trigonal copper coordination. The coordination of cuprous–thiolate species will have a greater covalency than nitrogen or oxygen coordination, and the corresponding filling of the Cu 4p orbitals would reduce the intensity of the 8984-eV peak. This provides a possible explanation of the lack of increased intensity of the 8984-eV peak for Cu_5S_7 and Cu_5S_6 with respect to Cu_4S_6. A further cause of reduction in intensity of this peak in the digonal case, which Kau *et al.*[36] investigated, is the T-shaped coordination in which another species interacts with the metal orthogonally to the two ligands. Although there is no structural evidence for unusually short interionic interactions in the model compound crystals,[23,26,37] there is some evidence for intracluster interactions which could well affect the edge spectra. The digonal S–Cu(I)–S species all show a slight displacement of the copper toward the center of the cluster (the angle S–Cu–S is 175.2° for Cu_5S_7, and the mean is 170.1° for the three angles in Cu_5S_6). Similarly, there is local distortion of up to 20° in the S–Cu–S angles at some of the trigonal sites in all three compounds. For the digonal coppers in Cu_5S_6, the closest Cu–Cu contacts are two trigonal coppers at about 2.7 Å and two digonal coppers at about 3.2 Å. The presence of coppers at these distances may influence the unoccupied energy levels. The presence of Cu–Cu contacts for trigonal copper at around 2.7 Å suggests that Cu–Cu contacts may also be significant for the interpretation of the edge spectra in this case. Deviations from ideal planarity and linearity will also change unoccupied energy levels, causing splitting and hence reducing the apparent intensity of the transition. The deviation from the ideal geometry also causes greater mixing of Cu 4s orbitals with the Cu 4p orbitals, making the transition less allowed. Finally, the cuprous–thiolate clusters contain several occurrences of Cu(I), each in a crystallographically distinct environment, with corresponding subtle variations in electronic structure. These small differences might cause the spectral features to become broadened (smeared out) and thus less intense. There are thus several possible causes for a lowering of the 8984-eV 1s → 4p peak intensity, and probably all have some effect.

In any case, setting theoretical arguments aside, it is clear from our results that the intensity of the 8984-eV transition in Cu K-edge spectra is not a good measure of the presence of digonal Cu(I) in copper(I)–thiolate cluster compounds. We therefore chose to investigate whether the Cu–S distance, which can be accurately determined from the EXAFS, could be used to determine digonal Cu(I).

Cu K-Edge EXAFS of Synthetic Cuprous–Thiolate Clusters. The copper K-edge EXAFS spectra of Cu_4S_6, Cu_5S_7, and Cu_5S_6 are shown in Figure 3A, together with the results of EXAFS curve-fitting analyses, and the corresponding Fourier transforms in Figure 3B. The Fourier transforms all have two main peaks, indicating that the EXAFS is dominated by two prominent interactions. The transform peak at around 2.2 Å is due to the Cu–S interactions, while the peak at around 2.7 Å is predominantly due to Cu–Cu interactions. The Cu–Cu peak varies more in magnitude with the cluster composition than the Cu–S contact. For the Cu_5S_6 EXAFS, trace contamination by zinc (Zn K-edge around 9660 eV, or k = 13.1 Å^{-1}) caused truncation of the data at k = 13 Å^{-1}, compared with a maximum of 15 Å^{-1} in the other two data sets. An even smaller trace of zinc in the Cu_5S_7 sample manifests itself in the small feature around 13.1 Å^{-1}, but this does not adversely affect the fitting in this case.

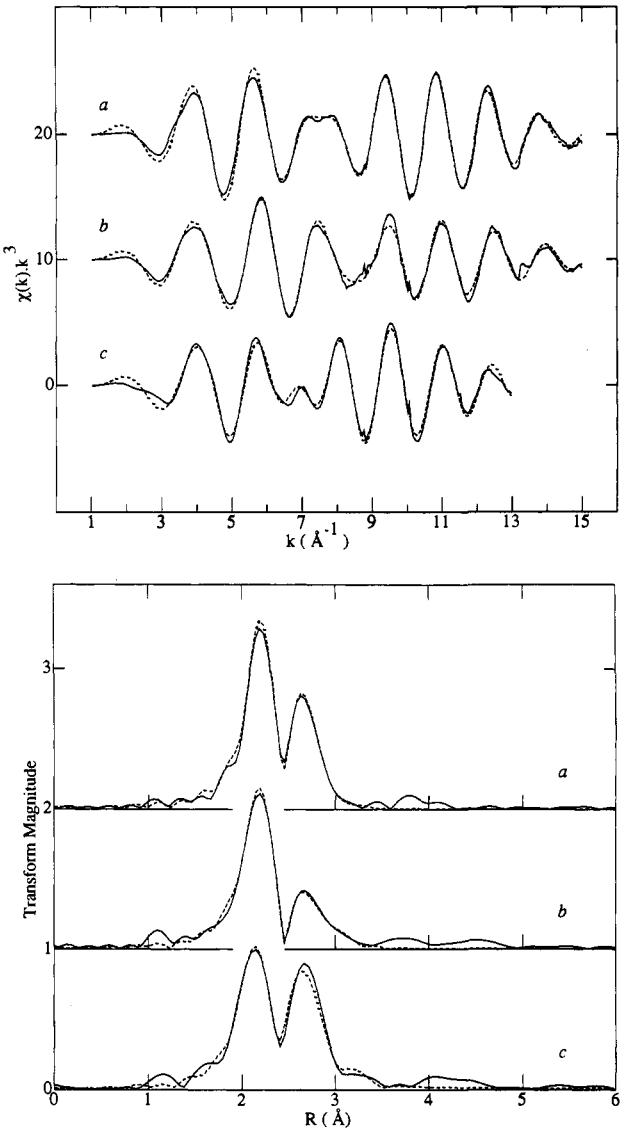

Figure 3. Cu K-edge EXAFS (A, top) and Fourier transforms (B, bottom) of synthetic copper(I)–thiolate cluster model compounds: (a) Cu_4S_6; (b) Cu_5S_7; (c) Cu_5S_6. The solid lines show the k^3-weighted raw EXAFS data, and the dashed lines the results of the fits as shown in Table I. Fourier transforms (here, and also below) were phase-corrected for Cu–S EXAFS.

As noted above, Cu_5S_7 and Cu_5S_6 contain both trigonal and digonal copper. The crystal structures of all three models[21,23,25,26] (Figure 1) indicate an average trigonal Cu–S bond distance of 2.28 Å and an average digonal Cu–S bond distance of 2.16 Å. Thus, the Cu–S bond length is around 0.12 Å longer for trigonal copper than for digonal copper. The limit of resolution for unfiltered EXAFS data is approximately $\Delta R = \pi/2\Delta k$ (from eq

(35) Weininger, M. S.; Hunt, G. W.; Amma, E. L. *J. Chem. Soc., Chem. Commun.* **1972**, 1140–1141.
(36) Kau, L. S.; Spira-Solomon, D. J.; Penner-Hahn, J. E.; Hodgson, K. O.; Solomon, E. I. *J. Am. Chem. Soc.* **1987**, *109*, 6433–6442.
(37) Dance, I. G. *J. Chem. Soc., Chem. Commun.* **1976**, 68–69.

Table I. Results of Cu K-Edge EXAFS Curve Fitting of Copper(I)–Thiolate Cluster Model Compounds[a]

	compound; fraction of digonal Cu, x_{dig}; range in k refined (Å^{-1})		
	Cu_4S_6; 0; 1–15	Cu_5S_7; 0.2; 1–15	Cu_5S_6; 0.6; 1–13
		Cu–S	
N	3	2.8	2.4
R (Å)	2.282(2)	2.258(2)	2.229(3)
σ^2 (Å^2)	0.0045(2)	0.0055(2)	0.0065(4)
r_{cryst} (Å)[b]	*2.291*	*2.254*	*2.221*
σ_{stat}^2 (Å^2)[c]	*0.0009*	*0.0020*	*0.0034*
		Cu–Cu	
N	3[e]	0.8	2.4
R (Å)	2.741(3)[e]	2.696(6)	2.725(3)
σ^2 (Å^2)	0.0075(3)[e]	0.0050(6)	0.0067(3)
r_{cryst} (Å)[b]	*2.738*	*2.682*	*2.721*
σ_{stat}^2 (Å^2)[c]	*0.0019*	*0.0012*	*0.0003*
		Cu–Cu	
		2	1.2
R (Å)		3.025(14)	3.16(2)
σ^2 (Å^2)		0.014(2)	0.012(3)
r_{cryst} (Å)[b]		*3.012*	*3.232*
σ_{stat}^2 (Å^2)[c]		*0.0057*	*0.0021*
F_{fit}[d]	0.123	0.129	0.153

[a] Values in parentheses are the 95% confidence limits, estimated as 3 times the estimated standard deviations obtained from the diagonal elements of the covariance matrix. These indicate the precision (as opposed to accuracy) to which parameters are determined within the constraints of the model. The presence of systematic errors (sometimes called statistical bias) will give a poorer accuracy, with major contributions from lack of transferability of phase and amplitude functions. Typical worst-case accuracies are ±0.02 Å for R (with directly coordinated atoms) and ±25% for N and σ^2. [b] Values of r_{cryst} are the mean bond distances calculated from the respective crystal structures. [c] σ_{stat}^2 is the static contribution to the Debye–Waller factor ($\sigma_{tot}^2 = \sigma_{vib}^2 + \sigma_{stat}^2$) and is calculated from the crystal structure, using $\sigma_{stat}^2 = (\sum(r_i - r_0)^2/n$, where n is the number of bonds, the sum is over each bond distance r_i, and r_0 is the mean bond distance. [d] Goodness of fit parameter, defined as $F_{fit} = (\sum(\chi_o - \chi_c)^2k^6)/(n_{obs} - n_{var})$ where χ_o and χ_c are the observed and calculated EXAFS, respectively, and n_{obs} and n_{var} are the numbers of observations and variables, respectively. [e] Phase and amplitude functions for the Cu–Cu contacts calculated from this shell (see Experimental Section).

1), where Δk refers to the k range fitted, and a resolution limit of 0.13 Å is obtained for separating two discrete Cu–S shells using the Cu_5S_6 data set (ΔR = 0.11 Å for the other two model data sets). The trigonal Cu–S bond distance additionally shows a degree of scatter around the mean distance. Because of these considerations, we do not expect to be able to resolve the Cu–S EXAFS into two discrete Cu–S interactions, and this interaction is best treated as a single shell averaged over the digonal and trigonal Cu(I) contributions.

The average coordination number for the Cu–S shell can be calculated as $N = 3x_t + 2x_d$, where x_t and x_d are the fractions of Cu(I) ions in the cluster present in trigonal and digonal coordination, respectively. In the curve-fitting analysis, bond lengths and Debye–Waller factors were floated and the coordination values fixed at the calculated values. The results of the curve-fitting analyses for all three compounds are summarized in Table I. The mean interatomic distances (r_{cryst}) calculated from the crystal structures are also given in Table I. There is an excellent correspondence between the two techniques, with agreement in interatomic distance to better than 0.01 Å for all shells, with the sole exception of the small outer Cu–Cu shell for Cu_5S_6, which differs by 0.07 Å. As noted above, EXAFS from absorber backscatterer pairs that are separated by less than the EXAFS resolution ΔR were treated as a single (averaged) interaction in the fit, with a significant static contribution to the Debye–Waller factor, σ_{stat}^2. The value of σ_{stat}^2 is calculated from the distribution of bond distances in the crystal structure (*cf.* ref 38 and Table I). We observe a correlation between σ_{stat}^2 and the total Debye–Waller factor, σ_{tot}^2, obtained from the EXAFS curve-fitting analysis, with both values increasing with increased disorder of the interatomic distances. We calculate that a maximum σ_{stat}^2 is expected for a fraction of 0.6 digonal Cu(I) in the cluster, because for this value there are equal numbers of trigonal and digonal Cu–S bonds. If it is assumed that $\sigma_{tot}^2 = \sigma_{stat}^2 + \sigma_{vib}^2$, where σ_{vib}^2 is the vibrational contribution to the Debye–Waller factor, then values of 0.0036, 0.0035, and 0.0031 Å^2 for σ_{vib} are calculated for x_d = 0.0, 0.2, and 0.6, respectively. These values fall within the chemically expected range and follow the expected trend toward smaller values for shorter bond lengths. As Debye–Waller factors are notoriously difficult to quantify, the observed trend and the chemical sensibility of these values are most gratifying.

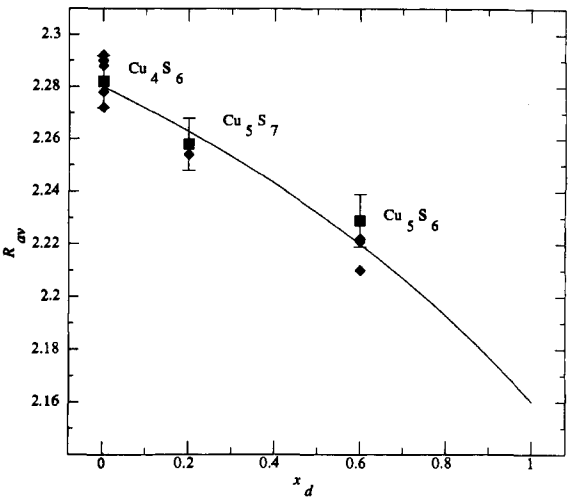

Figure 4. Mean copper(I)–sulfur bond distances as a function of the fraction of digonally coordinated copper. The points show (■) the results of EXAFS curve-fitting analyses of copper(I)–thiolate cluster model compounds (see Results and Table I) and (◆) the values of R_{av} for crystallographically characterized model compounds.[21-26,37] The line shows a predicted curve, assuming values of 2.28 and 2.16 Å for pure trigonal and digonal coordination, respectively.

The mean Cu–S bond distances deduced from the EXAFS analysis for the model cluster compounds show a systematic decrease with the fraction of digonal copper. Figure 4 shows these values for the three compounds, together with a predictive curve of the form

$$R_{av} = \frac{2x_dR_d + 3x_tR_t}{2x_d + 3x_t}$$

where x_d and x_t are the fractions of digonal and trigonal copper, respectively, and R_d and R_t are the corresponding Cu–S bond distances for exclusive digonal and trigonal coordination. The curve thus predicts the mean Cu–S bond distances, weighted appropriately. From a consideration of a variety of synthetic copper(I)–thiolate cluster crystal structure data with different thiolate ligands, values of 2.16 and 2.28 Å were chosen for R_d and R_t, respectively. It can be seen that excellent correlation is obtained between the observed bond distances and the curve. Thus, one may conclude that the mean Cu–S distance obtained from EXAFS may be used to measure the fraction of digonal copper in biological cuprous–thiolate clusters.

Cu K-Edge XAS of Cuprous–Thiolate Clusters in Metalloproteins. The data reported in this work comprise a reanalysis of some previously published data and new data on six different proteins: *S. cerevisiae* copper metallothionein, the *S. pombe* Cu–$(\gamma EC)_nG$ complex, synthetic Cu–$(\gamma EC)_nG$, synthetic Cu–$(\alpha EC)_nG$, CuACE1, and, of particular note, CuE7, an oncogenic DNA-

(38) For example, see: Teo, B. K. In *EXAFS: Basic Principles and Data Analysis*; Springer-Verlag: Berlin, Heidelberg, New York, Tokyo, 1986.

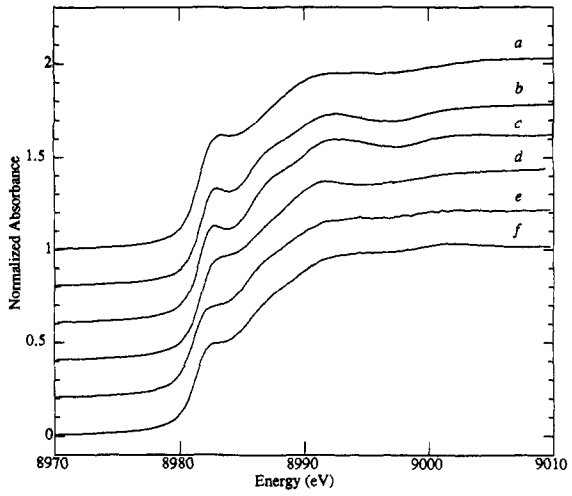

Figure 5. Cu K-edge absorption spectra of metalloproteins: (a) *S. cerevisiae* CuMT; (b) *S. pombe* Cu–$(\gamma EC)_nG$; (c) synthetic Cu–$(\gamma EC)_nG$; (d) synthetic Cu–$(\alpha EC)_nG$; (e) CuACE1; (f) *Papilloma* virus CuE7.

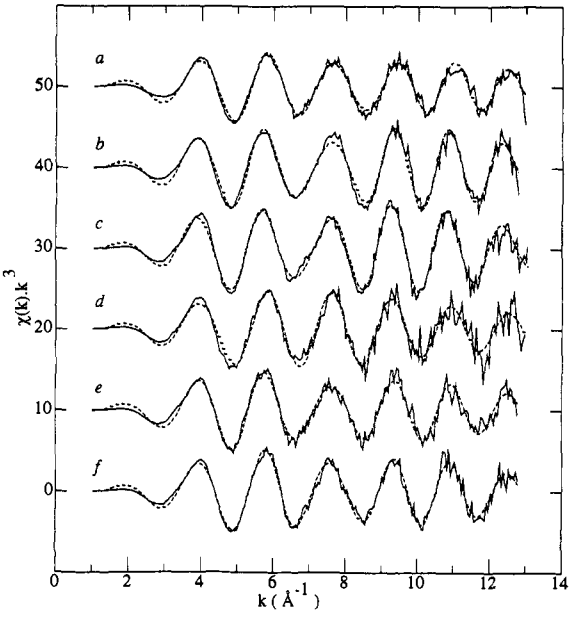

Figure 6. Cu K-edge EXAFS of metalloproteins: (a) *S. cerevisiae* CuMT; (b) *S. pombe* Cu–$(\gamma EC)_nG$; (c) synthetic Cu–$(\gamma EC)_nG$; (d) synthetic Cu–$(\alpha EC)_nG$; (e) CuACE1; (f) *Papilloma* virus CuE7. The solid lines show the k^3-weighted raw EXAFS data, and the dashed lines, the results of the fits as shown in Table II.

binding protein from the *Papilloma* virus. The edge spectra of the different metalloproteins are compared in Figure 5. It can be seen that all the spectra are very similar; all have a pronounced feature at about 8984 eV, and all show a strong similarity to the model compound copper–thiolate cluster spectra shown in Figure 2.

Cu K-edge EXAFS spectra of metalloprotein samples are shown in Figure 6, and the corresponding Fourier transforms, in Figure 7. The Fourier transforms have a form similar to those of the synthetic cluster compounds (Figure 3B). Each of the Fourier transforms shows a prominent first-shell Cu–S contact, and all samples except for the Cu–$(\alpha EC)_nG$ peptide additionally show a second, smaller contact which corresponds to the Cu–Cu shell. The presence of the Cu–Cu contact is indicative of the presence of a copper–thiolate cluster in these proteins.

EXAFS curve-fitting analyses were carried out on the metalloprotein samples. In these cases, the average coordination numbers for the copper centers are not known. An independent determination of average coordination number for an unknown cluster from EXAFS data is difficult, since there is a very high

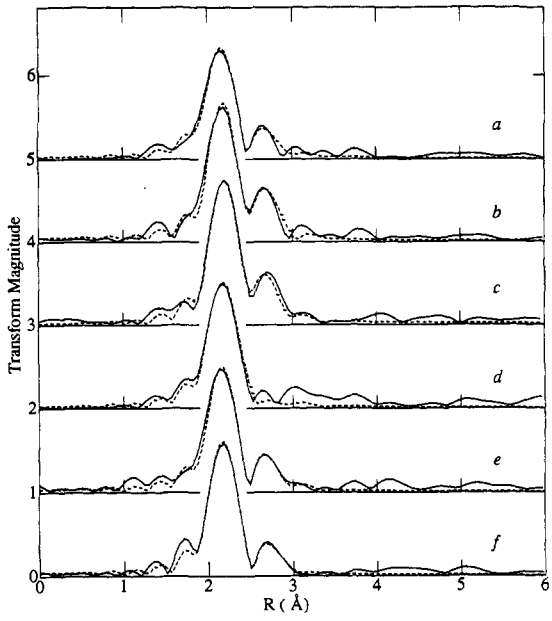

Figure 7. Cu K-edge EXAFS Fourier transforms of metalloproteins: (a) *S. cerevisiae* CuMT; (b) *S. pombe* Cu–$(\gamma EC)_nG$; (c) synthetic Cu–$(\gamma EC)_nG$; (d) synthetic Cu–$(\alpha EC)_nG$; (e) CuACE1; (f) *Papilloma* virus CuE7. The solid lines show the Fourier transform of the raw data, and the dashed lines, the results of the fits shown in Figure 6 and Table II.

correlation (generally >90%) between N and σ^2 for a particular shell. In order to estimate a coordination number for the Cu–S shell, the value of the coordination number was incremented in steps of 0.2, and a fit was carried out at each step with R and σ^2 of all shells floating. The coordination number corresponding to the best fit was then chosen and held constant. The estimates of coordination numbers thus obtained for the Cu–S shell lie in the range $2.6 \leq N \leq 3.0$, which, by analogy with the synthetic model clusters, is plausible. The corresponding Debye–Waller factors lie in the range $0.0038 \leq \sigma^2 \leq 0.0057$ Å^2, which again compare well with the values for the model compounds. The value of N for the Cu–Cu shells was chosen in a similar way, applying an increment of 0.5 in N. In each case the presence of two Cu–Cu shells, the first at around 2.7 Å and the second at 3.0–3.0 Å, was tested, but only in the case of the CuE7 protein from the *Papilloma* virus was a significant improvement in the fit obtained by the addition of an extra shell. In this case, the Cu–Cu peak in the Fourier transform (Figure 7) contains contributions from the two Cu–Cu interactions (as with the Cu_5S_6 and Cu_5S_7 models (Figure 3B)). Previously, in the case of *S. cerevisiae* copper metallothionein, very high quality data allowed an additional Cu–Cu shell at 4.02 Å to be observed; this was not observed in the present data due to the somewhat poorer signal to noise ratio. The results of the EXAFS curve fitting are given in Table II.

The predictive curve of Figure 4 was then used to estimate the fraction of digonally coordinated Cu(I) present in the cuprous–thiolate metalloprotein clusters, using the mean Cu–S distance as obtained from EXAFS curve-fitting analysis. The results are shown in Table III and include the analysis of new data, together with some reanalysis of previously published EXAFS data,[2,39] using the same phase and amplitude functions used in the EXAFS analysis of the model compounds (see Experimental Section). Also included are the predictions for two proteins from other workers;[40,41] however, as these values were obtained using different

(39) Smith, T. A.; Lerch, K.; Hodgson, K. O. *Inorg. Chem.* **1986**, *25*, 4677–4680.
(40) Abrahams, I. L.; Bremner, I.; Diakun, G. P.; Garner, C. D.; Hasnain, S. S.; Ross, I.; Vasak, M. *Biochem. J.* **1986**, *236*, 585–589.
(41) Freedman, J. H.; Powers, L.; Peisach, J. *Biochemistry* **1986**, *25*, 2342–2349.

Table II. Results of Cu K-Edge EXAFS Curve Fitting of Metalloproteins

metalloprotein	interaction	N	R (Å)	σ^2 (Å^2)	k_{max} (Å^{-1})	F_{fit}[a]
S. cerevisiae CuMT	Cu–S	2.8	2.250(4)	0.0056(5)	13.0	0.368
	Cu–Cu	0.5	2.703(11)	0.0028(10)		
S. pombe Cu–$(\gamma EC)_nG$	Cu–S	3.0	2.270(3)	0.0041(4)	12.8	0.487
	Cu–Cu	1.5	2.747(8)	0.0059(8)		
synthetic Cu–$(\gamma EC)_nG$	Cu–S	3.0	2.278(3)	0.0034(3)	13.0	0.471
	Cu–Cu	2.5	2.768(10)	0.0101(11)		
synthetic Cu–$(\alpha EC)_nG$	Cu–S	2.8	2.257(5)	0.0042(6)	13.0	1.05
CuACE1	Cu–S	2.8	2.258(4)	0.0043(4)	12.8	0.533
	Cu–Cu	3.0	2.717(15)	0.014(2)		
Papilloma virus CuE7	Cu–S	2.8	2.263(3)	0.0038(3)	12.8	0.402
	Cu–Cu	2.0	2.72(2)	0.014(3)		
	Cu–Cu	0.5	3.07(4)	0.008(5)		

[a] Goodness of fit parameter, defined as $F_{fit} = (\sum(\chi_o - \chi_c)^2 k^6)/(n_{obs} - n_{var})$, where χ_o and χ_c are the observed and calculated EXAFS, respectively, and n_{obs} and n_{var} are the numbers of observations and variables, respectively.

Table III. Fractions of Digonal Cu(I) in Copper–Thiolate Clusters of Metalloproteins

metalloprotein	R (Å)	predicted x_d
S. cerevisiae CuMT[2a]	2.242[a]	0.4
S. cerevisiae CuMT	2.250	0.3
N. crassa CuMT[39]	2.233[a]	0.5
rat CuMT-β[2b]	2.255[a]	0.3
pig CuMT[40]	2.25[b]	0.3
dog CuMT[41]	2.27[b]	0.1
S. pombe Cu–$(\gamma EC)_nG$	2.270	0.1
synthetic Cu–$(\gamma EC)_nG$	2.278	0.0
synthetic Cu–$(\alpha EC)_nG$	2.257	0.3
CuACE1	2.258	0.3
Papilloma virus CuE7	2.263	0.2

[a] EXAFS data for these proteins have been reevaluated using the same phase and amplitude functions as employed in this work. [b] Values of R for these proteins have been taken from the literature; in this case, the systematic difference between the EXAFS phases and amplitudes means that the estimated value for x_d must be considered less accurate.

phase and amplitude functions compared with those used to generate Figure 4, the estimate of the fraction of digonal Cu(I) may be less reliable. The values for x_d shown in Table III vary from 0.0 (*i.e.* pure trigonal copper) to 0.5.

Discussion

We have previously reported copper K-edge and sulfur K-edge EXAFS analyses of copper metallothionein from *S. cerevisiae*.[2] The Cu–S distances determined for the wild-type metallothionein and two truncated mutant proteins were all close to 2.24 Å.[2] Reanalysis of the original wild-type EXAFS data by curve fitting using the current, much improved, phase and amplitude functions yielded a best fit with a mean Cu–S distance of 2.242 Å and a mean coordination number of 2.6, in excellent agreement with the original analysis. We also collected new EXAFS data on a second yeast copper metallothionein isolate (Table II), although in this case trace zinc contamination limited the maximum k to 13 Å^{-1}. A marginally longer mean Cu–S distance of 2.250 Å was obtained with this new data set. A comparison of these mean Cu–S distances to the results for the synthetic cuprous–thiolate clusters in Figure 4 predicts a fraction of digonal Cu(I) ions in *S. cerevisiae* copper metallothionein of 0.3–0.4 (see Table III). This value is consistent with the likely fraction of digonal Ag(I) of $^2/_7$ determined by HMQC NMR measurements of silver metallothionein.[3] For both data sets, a well-defined second shell of Cu–Cu contacts was indicative of the presence of a multimetallic cuprous–thiolate cluster. Data from several other metallothioneins are also included in Table III, and these show a variation of the predicted fraction of digonal copper between 0.1 and 0.5.

X-ray absorption studies were performed on *in vivo* produced Cu–$(\gamma EC)_nG$ peptide complexes from *S. pombe* and synthetically produced Cu–$(\alpha EC)_nG$ and Cu–$(\gamma EC)_nG$ complexes. The isopeptides, $(Glu–Cys)_nGly$, differ from glutathione in having multiple (Glu–Cys) dipeptide units with $2 \leq n \leq 6$.[5] The complexes are oligomers of undefined M_r so that the precise Cu(I) stoichiometry is uncertain, although four to six ions per complex seem likely.[5] Mean Cu–S bond distances of 2.270, 2.278, and 2.257 Å were determined by EXAFS curve fitting for *S. pombe* Cu–$(\gamma EC)_nG$, synthetic Cu–$(\gamma EC)_nG$, and synthetic Cu–$(\alpha EC)_nG$, respectively (Table II). Using the correlation of Figure 4, these distances indicate a close to exclusive trigonal coordination of the Cu(I) by sulfur in the Cu–$(\gamma EC)_nG$ complexes but a significant fraction of digonal copper (0.3) in the case of the Cu–$(\alpha EC)_nG$ complex. For the Cu–$(\gamma EC)_nG$ complexes, clearly defined Cu–Cu interactions, apparent in the outer shell at 2.75 Å, indicate multimetallic copper–thiolate clusters. The EXAFS of the native and synthetic Cu–$(\gamma EC)_nG$ complexes were found to be quite similar, although the curve fitting gave a larger N for the Cu–Cu interaction in the synthetic complex. We were not able to observe a Cu–Cu interaction in the Cu–$(\alpha EC)_nG$ EXAFS. Nevertheless, the presence of a cluster seems highly probable.[5] It seems possible that the slightly lower signal to noise ratio of these data, perhaps combined with some heterogeneity in the Cu–Cu distances, makes the Cu–Cu interaction unobservable in this case.

In previous work, we have reported Cu K-edge X-ray absorption studies on the N-terminal half of the ACE1 polypeptide as a Cu(I) complex, both as CuACE1 purified from a bacterial expression system and as CuACE1 prepared by *in vitro* reconstitution protocols from the apoprotein.[9,10] The CuS cluster in CuACE1 contains six to seven copper atoms.[9] The edge spectrum of CuACE1 was observed to be dominated by an edge feature near 8983 eV, very similar to that seen in the spectrum of copper metallothionein. Partly on the basis of the model compound data of Kau *et al.*,[36] the conclusion was reached that the Cu(I) ions were predominantly trigonal.[9,10] New data have been recorded for CuACE1 prepared by *in vitro* reconstitution using Cu–glutathione as the Cu(I) donor (Figures 5–7). Curve-fitting analysis of the EXAFS of CuACE1 (Figure 7, Table II) reveals a mean Cu–S bond distance of 2.258 Å, which is very similar to that found in our previous work[9,10] (Table II). The correlation in Figure 4 suggests that the stoichiometry of CuACE1 may be represented by one to two digonal and four to five trigonal Cu(I) ions. As with metallothionein, the presence of a cluster in CuACE1 is indicated by the Cu–Cu interactions apparent in the EXAFS, which, at 2.72 Å, are similar to the short Cu–Cu distances observed in copper metallothioneins and synthetic trigonally coordinated copper–thiolate clusters. The Cu–Cu outer shell is much better defined in the present CuACE1 data than is the case for both ACE1 prepared by reconstitution in the absence of glutathione[9] and native yeast copper metallothionein.

The E7 protein from *Papilloma* viruses is a metalloprotein. The identity of the metal ion populating the binding site in virally

infected cells is unclear, but expression of E7 genes from human HPV16 *Papilloma* and rabbit *Papilloma* viruses in an *E. coli* expression system yields E7 protein as a ZnE7 protein complex.[15,16] The Zn(II) ions in the E7 proteins undergo a rapid metal-exchange reaction with Cu(I) ions, yielding CuE7 proteins with stoichiometries of 2 and 3 mol equiv for HPV16 and rabbit *Papilloma* virus CuE7s, respectively.[15] X-ray absorption spectroscopy on rabbit *Papilloma* virus CuE7 revealed a mean Cu–S distance of 2.265 Å and the presence of a Cu–Cu scatter peak indicative of a multimetallic Cu–S cluster. As CuE7 contains only 3 mol equiv of Cu(I), any digonally coordinated Cu(I) ions would be expected to be more clearly evident in the mean Cu–S distance compared to those of copper–thiolate clusters of higher nuclearity. Data are most consistent with exclusively trigonal Cu(I) coordination.

Conclusion

The identification of the coordination geometry within a given cuprous–thiolate multimetallic cluster is a difficult problem. The Cu K-edge X-ray absorption data, together with careful analyses of Cu–S bond distances from EXAFS, appear to be the best spectroscopic indicator in the absence of other structural data. From the Cu(I)–thiolate synthetic model compounds discussed here, it appears that the mean Cu–S bond distance is a significantly better indicator than the nature of the 8983-eV edge feature in the edge spectrum.

Acknowledgment. We thank Professor Keith Hodgson for the *Neurospora crassa* metallothionein EXAFS data and also for helpful discussions. We thank Dr. Roger Prince and Yeunjong Gea for assistance with data collection. We are indebted to our colleagues on the staff of the Stanford Synchrotron Radiation Laboratory (SSRL) for their assistance. SSRL is operated by the Department of Energy, Office of Basic Energy Sciences. Support for research by SSRL staff is provided by that Office's Division of Materials Science. The SSRL Biotechnology Program is supported by the National Institutes of Health, Biomedical Resource Technology Porgram, Division of Research Resources. Further support is provided by the DOE, Office of Health and Environmental Research. We also thank Dr. Garry S. H. Lee for preparation of model compounds. D.R.W. is supported by the National Institutes of Health (Grant ES 03817), and C.T.D. is supported by Training Grant T32 AM 07115 from the National Institutes of Health.

Supplementary Material Available: A table of EXAFS Cu–Cu phase and amplitude functions (4 pages). Ordering information is given on any current masthead page.